The effects of re-irradiation on the chemical and morphological properties of permanent teeth.

Thais Tedeschi Santos
Universidade de São Paulo
Vicente Silva Mattos
Universidade de São Paulo
Kelly Fernanda Molena
kelly.molena@usp.br
Universidade de São Paulo
Francisco Wanderley Garcia de Paula e Silva
Universidade de São Paulo
Harley Francisco de Oliveira
Universidade de São Paulo
Juliana Jendiroba Faraoni
Universidade de São Paulo
Paulo Nelson Filho
Universidade de São Paulo
Jarbas Caiado de Castro Neto
Universidade de São Paulo
Regina Guenka Palma-Dibb
Universidade de São Paulo
Alexandra Mussolino de Queiroz
Universidade de São Paulo

Research Article

Keywords: Head and neck neoplasia, Radiotherapy, Enamel, Dentin, Chemical composition, Morphology

Posted Date: November 17th, 2023

DOI: https://doi.org/10.21203/rs.3.rs-3613368/v1

Additional Declarations: No competing interests reported.

Version of Record: A version of this preprint was published at Radiation and Environmental Biophysics on April 16th, 2024. See the published version at https://doi.org/10.1007/s00411-024-01068-1.

Abstract

Objectives

Evaluate in vitro, simulating a radiotherapy retreatment of HNC, the effects of re-radiation on the properties of enamel and dentin.

Materials and Methods

Forty five human permanent molars were divided in five groups: non-irradiated; irradiated up to a dose of 60 Gy and re-irradiated up to doses of 30, 40 and 50 Gy, through the analysis of Raman spectroscopy, Scanning electron microscopy (SEM) and Energy Dispersive X-ray spectroscopy (EDS). Raman spectroscopy was analyzed comparatively, according to the intensity, general area of the spectra and peaks of interest. Kolmogorov – Smirnov test, followed by the One-Way ANOVA test and Tukey's post-test, with the significance level were adopted for all analyzes being 5%.

Results

There were significant changes in the peaks of irradiated, non-irradiated and re-irradiated enamels, with the presence of phosphate (438nm), hydroxyapatite (582nm), phosphate (960nm) and carbonate (1070nm) ($p < 0.05$). Re-irradiation reached the tooth as a whole ($p > 0.05$), with degradation of the interprismatic region, destruction of enamel prisms and hydroxyapatite crystals. In dentin, it caused obliteration of the tubules, formation of cracks and progressive fragmentation of collagen fibers. EDX indicated an increase in the percentage of oxygen and a decrease in phosphorus and calcium after re-irradiation.

Conclusion

The chemical and morphological changes in the permanent irradiated teeth are progressive and directly proportional to the escalation of the radiation dose.

Clinical relevance

Re-irradiation causing even more damage to enamel and dentin of permanent teeth.

INTRODUCTION

Radiotherapy (RT) is an option for the treatment of Head and neck cancer (HNC). Protocols based on dose fractionation are used [1–3], due to potential of higher doses of RT cause severe tissues damage [4,5].

Locoregional recurrence of HNC can occur, which can impact the quality of life of these patients and their parents [6–8]. In this case, treatment is performed as a second attempt at cure. The addition of therapies, can cause toxicity to adjacent tissues in a more complex way, with side range from 13 to 89%

[9]. The most common complications caused by RT in HNC are mucositis [10], xerostomia, candidiasis, dysgeusia, trismus [11], orofacial pain, changes in the periodontal ligament [12], microvascular changes, soft tissue necrosis, osteoradionecrosis [13] and radiation-related caries (RRC) [14–21].

RT effects depend on the mineral and organic composition of the enamel or dentin [14,22]. Studies involving permanent teeth have shown that RT is capable of causing changes in the enamel [23,24,25,26] and dentin [16,18,19,23–26], such as destruction of the prismatic structure of enamel [27] and alteration in mechanical and chemical properties [23–25,27–37].

Although the direct changes that RT can promote in dental structures are known, there is no report in the literature on the influence of RT on the chemical and morphological properties of dental tissues in cases of patients undergoing a new radiotherapy treatment, that is, in cases of re-irradiation, after locoregional recurrence of HNC, this assessment being the objective of the present study.

MATERIAL METHODS

Ethical aspects and sample

The research was approved by the Research Ethics Committee (process no. 2018.3.091.548).
This is an experimental study taking irradiation at 5 levels as a factor:

1) G1: Not irradiated (control);

2) G2: Irradiated up to a dose of 60Gy (conventional);

3) G3: Re-irradiated up to a dose of 30Gy (irradiated up to a dose of 60Gy and re-irradiated up to a dose of 30Gy);

4) G4: Re-irradiated up to a dose of 40Gy (irradiated up to a dose of 60Gy and re-irradiated up to a dose of 40Gy);

5) G5: Re-irradiated up to a dose of 50Gy (irradiated up to a dose of 60Gy and re-irradiated up to a dose of 50Gy).

The sample consisted of 45 human permanent molars [23,30,32,33,38–40], recently extracted and healthy. The teeth were cleaned, disinfected and stored in a supersaturated 0.1% thymol solution for one week. They are then washed in water for 24 hours and stored in distilled water at 4ºC for a month.

The dental substrates of enamel and coronal dentin were analyzed separately and were not compared with each other. The specimens were subjected to chemical and structural composition analysis (Raman). Four specimens from each group were randomly separated for analysis using scanning electron microscopy (SEM) and evaluation of the chemical composition of enamel and dentin using energy dispersive X-ray spectroscopy (EDS).

Irradiation and re-irradiation process

Irradiation process

The specimens were irradiated at the Radio-Oncology Treatment Center, Ribeirão Preto, Brazil. During the irradiation procedure, the specimens were placed in 24-well acrylic cell culture plates (Cellstar®, ref.657160, Greiner bio-one GmbH, Frickenhausen, Germany), so that they all received the same direct irradiation by area [23] (Fig. 1).

Initially, the teeth (G2) were subjected to irradiation in a linear accelerator (Fig. 1A-E) with energy of 6MV, dose of 60Gy, in a total of 30 fractions for six weeks, in a dose fraction of 2Gy/day, for five consecutive days per week [23–26,30,33,35–37,40–43].

Storage and accelerated artificial aging

After the conventional irradiation process (total dose of 60Gy) (G2), the teeth were stored in artificial saliva at 37ºC (± 1ºC), for six months. During this period, all specimens were subjected to accelerated artificial aging through thermocycling, in order to simulate a period of one year, a time suggested in the literature as the minimum necessary to initiate a new radiotherapy treatment [44].

Re-irradiation process

After the storage period, following the initial irradiation procedure, the teeth were subjected to re-irradiation up to a total dose of 30Gy (G3), 40Gy (G4) and 50Gy (G5) according to their group, in a total of 15 fractions for 3 weeks, 20 fractions for 4 weeks and 25 fractions for 5 weeks, respectively, in a dose fraction of 2 Gy/day, for 5 consecutive days per week.

Assessment of the chemical composition of enamel

Raman Spectroscopy

After irradiation process, all specimens were analyzed by Raman spectroscopy (Ocean Optics spectrometer, Inc., Dunedin, FL, USA), with diode laser excitation (λ = 785nm), spectral resolution of 11cm^{-1}, with excitation power at 400mW, five seconds of acquisition and three acquisitions in each region, with the final spectrum of each region being the average of each of these three measurements (Fig. 1F-H).

Each sample provided a total of six spectra, named according to the group and region analyzed. The regions analyzed in each samples were:

- **CE_V**: Coronary Enamel – Vestibular Face;
- **CE_L**: Coronary Enamel – Lingual/Palatal Face;
- **BS**: Bottom sulcus;

- **TC**: Tip Cuspid;
- **ADJ_V**: Amelodentinal Junction – Vestibular Face;
- **ADJ_L**: Amelodentinal Junction – Lingual/Palatal Face;

All spectra were processed using a MatLab processing routine that involves:

- Noise removal to smooth the curve;
- Removal of base curve using polynomial of order six;
- Removal of second order oscillations inside the curves;
- Definition of peaks of interest;
- Lorentzian plot with maximum at the peak of interest;
- Calculation of the area of each peak of interest;
- Calculation of the intensity of each peak of interest;
- Calculation of the total spectrum area.

The peaks selected for analysis were [45–47]:

- 438nm: Peak related to phosphate presence;
- 582nm: Vibrational mode v1, v3 and v4 $(PO_3)^{-4}$ in hydroxyapatite;
- 960nm: Symmetrical vibrational stretching of phosphate ions ($(PO_4)^{-3}$);
- 1070nm: Peak related to carbonate presence.

Furthermore, analysis of the carbonate/phosphate ratio was also carried out, by analyzing the ratio between the values obtained for both peaks.

Morphological analusis of enamel and dentin

Scanning electron microscopy (SEM)

Four dental hemisections were used from each group (20 hemisections) [24].

They were then observed under a scanning electron microscope (Philips, São Paulo, Brazil)) with a magnification of 500x and 2000x. The areas analyzed correspond to the entire thickness of the enamel and dentin (morphological and qualitative comparison).

Raman Spectroscopy

For this analysis, no prior sample is not necessary, one of its great advantages is that it is a non-invasive and non-destructive technique.

Chemical analysis of enamel and dentin

Energy-Dispersive X-ray Spectroscopy (EDS)

Four dental hemisections from each group (20 hemisections), were subjected to chemical analysis using EDS (ZEISS, SIGMA scanning electron microscope - equipped with field emission electron gun (SEM-FEG) and OXFORD qualitative and quantitative chemical analysis system for detection of elements between Boron and Uranium - Electronic Microscopy and Laboratory Analysis, São Carlos Physics Institute, University of São Paulo, IFSC-USP, São Carlos, São Paulo, Brazil).

The sample was irradiated with an X-ray beam of 50μm radius, tube voltage of 50kV, with automatic current adjustment, and a beam diameter of 50μm. Measurements were carried out for 100 seconds per point.

For each sample, the mapping of the components calcium (Ca), oxygen (O) and phosphorus (P), in a line of 40x1 points, steps of 10μm, 50kV, in real acquisition time (one second per point), with a final scanning time of 36 minutes per sample. In all measurements, radiation was counted using a Si (Li) semiconductor detector cooled by liquid nitrogen. The synthetic stoichiometric hydroxyapatite reagent (Sigma-Aldrich; Sintra, Portugal, purity 99.99% [$Ca_5HO_{13}P_3$]) was used as a reference for calibration. The spectra corresponding to each sample were processed using the EDS Software (PCMEDX V.1.04 Shimadzu Cor., Kyoto, Japan). For descriptive analysis of the data, the concentration by weight of the elements Ca, P and O was used.

Data analysis

Raman spectroscopy was analyzed comparatively, among themselves and by region according to the general area of the intensity and peaks. Data were evaluated using the Kolmogorov–Smirnov test, presenting a normal distribution. Comparison between groups was performed using One-Way ANOVA test and Tukey's post-test, with a significance level of 5% and using GraphPad Prism ® 5 Software (GraphPad Software In., San Diego, California, USA).

SEM images were analyzed through qualitative comparison of the different experimental conditions.

The data relating to the concentration by weight of the elements Ca, P and O, obtained by EDS, were subjected to comparative percentage analysis.

RESULTS

Raman Spectroscopy

Processing each spectrum, separating it according to groups and obtaining the averages for each region resulted in the spectra presented in Fig. 2.

The first parameter to be observed was the total spectra areas (Fig. 3). It was possible to observe a tendency for the total areas of the graphs to increase, that it indicates the occurrence of consistent

structural and chemical changes within.

Statistically significant difference between the groups ($p < 0.05$) (Fig. 3), and for G5, this change was even more significant. Statistical analysis of the data was performed, for each of the peaks (Fig. 3).

When analyzing the presence of phosphate (438nm), although it is possible to observe changes statistically significant only between the non-irradiated and irradiated groups, in relation to G3 ($p < 0.05$) (Fig. 4A1).

Data obtained by the areas of the peaks related to the hydroxyapatite (582nm), phosphate ion (960nm), and carbonate (1070nm), allowed to observe statistical difference between the groups ($p < 0.05$), and changes were more relevant in G3 and G5 (Fig. 4B, 4C1 and 4D1).

When analyzing the phosphate (438nm) peak and the vibrational modes of hydroxyapatite (582nm), the groups showed a statistically significant difference between them ($p < 0.05$), and the groups with the most relevant changes were those G3 and G5 (Fig. 4A2 and 4B2).

Intensities of the phosphate ion peak (960nm) indicating possible structural and chemical changes within the samples, these changes were statistically significant only among the group of non-irradiated teeth in relation to G5 ($p < 0.05$) (Fig. 4C2).

In relation to the intensity of the carbonate peak (1070nm), G5 showed statistically significant differences when compared to all other groups, as well as the elements of the non-irradiated group, in relation to G3 ($p < 0.05$) (Fig. 4D2).

The analysis of the intensity of the peaks at 960nm (phosphate ions) and 1070nm (carbonate) between them, demonstrates a tendency towards an increase in the carbonate/phosphate ratio (1070/960) with the increase in radiation doses, in all the analyzed regions (Fig. 5A1). There was no statistically significant difference between the regions ($p > 0.05$) (Fig. 5A2).

Scanning electron microscopy (SEM)

The images obtained by SEM showed progressive morphological changes in both enamel and dentin, with the escalation of radiation doses.

Enamel

Morphological analysis of the non-irradiated (G1) teeth presented well-organized prisms surrounded by interprismatic regions (Fig. 6A1 and 6A2).

After irradiation (G2), changes were observed on the surface of this tissue, in all regions analyzed, at different magnifications. The interprismatic portion became more evident, and it was possible to identify the prisms enamel and crystals (Fig. 6B1 and 6B2).

After the re-irradiation procedure, in G3, G4 and G5, the specimens showed progressive morphological changes, with different magnifications, loss of evidence of the interprismatic region and difficulty in observing the prisms and crystals (Fig. 6C1–6E2).

Dentin

The non-irradiated teeth had well-defined dentinal tubules and a well-organized collagen fiber network (Fig. 7A1 and 7A2).

In G2, changes in the intertubular, peritubular and intratubular dentin can be observed, and at the 20000x magnification, cracks in the dentin structure and obstruction of the dentinal tubules. Regarding the collagen fibers, there is a lack of structure, and at a magnification of 20,000x it was possible to verify their fragmentation (Fig. 7B1 and 7B2).

After re-irradiation process, in G3, G4 and G5, the specimens showed progressive changes, as the radiation dose increased, with degradation of the intertubular, peritubular and intratubular structure, presence of cracks throughout the dentin structure, obliteration of the tubules and degradation of the collagen fiber network (Fig. 7C1-7E2).

Energy-Dispersive X-ray Spectroscopy (EDS)

The percentages of the chemical elements oxygen (O), phosphorus (P) and calcium (Ca) in the enamel and dentin of teeth in G1, G2, G3, G4 and G5 were analyzed (Table 1).

Table 1
Average percentage of chemical elements present in the enamel and dentin of non-irradiated (G1), irradiated up to 60 Gy (G2) and re-irradiated up to 30 Gy (G3), 40 Gy (G4) and 50 Gy (G5).

Enamel					
Elements	**G1**	**G2**	**G3**	**G4**	**G5**
Oxygen (O)	37,09	38,95	45,4	47,8	49,4
Phosphorus (P)	19,13	18,55	14,5	13,5	13,5
Calcium (Ca)	42,95	42,37	29,7	26,8	26,4
Dentin					
Elements	**G1**	**G2**	**G3**	**G4**	**G5**
Oxygen (O)	36,47	38,05	40,8	44,5	45,3
Phosphorus (P)	19,17	19,05	12,9	11,3	11,2
Calcium (Ca)	42,83	42,56	25,9	22,7	22,06

According to the data, when compared to G1 were an increase in the percentage of oxygen in G2, and becomes even more evident in G3, G4 and G5. However, the percentage of phosphorus and calcium in enamel and dentin after 60Gy of irradiation decreased and were even more lower with the increased of irradiation dose.

DISCUSSION

In the present study, after the first cycle of radiation morphological changes were observed in the enamel compared to the non-irradiated sample. In re-irradiated specimens, with the escalation of radiation dose, the changes became even more evident [27,29,31].

Analysis of the area and intensity of the phosphate peaks, demonstrate that RT is affect the mineral and crystalline structure. Analyzing hydroxyapatite peaks (582nm) and carbonate (1070nm), as well as the carbonate/phosphate ratio, the results suggest the occurrence of the hydroxyl substitution process of hydroxyapatite ($Ca_{10}(PO_4)_6OH_2$) by carbonate, with a consequent increase in the solubility of dental enamel and dissolution of enamel crystals, favoring the demineralization process. Also altering the crystal dimensions, surface texture and stability of the hydroxyapatite, causing damage to this tissue that is even more severe with the re-irradiation process. Similarly, studies suggest that are loss of protein post radiation [14,46,48] and mineral [46,48]. It is important to clinical consideration about the use of fluoride to prevent RRC post-radiotherapy and mainly post re-irradiation therapy [48].

There is a tendency for the carbonate/phosphate ratio (1070/960) to increase with increasing radiation doses in all regions, regardless of the region analyzed, re-irradiation is not more damaging to one region than the other, but rather affects the tooth structure as a whole. Others studies suggest that this damages are even higher in cement-enamel junction [14,46].

It was possible to observe degradation of the interprismatic region and destruction of the enamel prisms and hydroxyapatite crystals, in SEM images. In dentin, indicated obliteration and degradation of the intertubular, peritubular and intratubular structure, presence of cracks and degradation of the collagen fiber [24,30,49]. Grötz et al. (1997) [27] attributed the obliteration of dentinal tubules, to the degeneration of the odontoblastic processes, being the result of direct radiogenic damage to the cells. The dentin acts as support for the enamel, and if its structure is compromised, it is possible that this support becomes less efficient, contributing to the occurrence of enamel fractures and cracks [46].

In order to observe the behavior of some elements were used EDS. In the irradiated enamel, after the 60Gy dose, a slight increase in the oxygen and a small decrease in the phosphorus and calcium were observed. These variations became even greater and more evident when analyzing the re-irradiated specimens. The decrease in the amount of calcium and phosphorus observed may be due to changes in the solubility of enamel after irradiation. This tissue would lose ions to the environment, differently of other studies [50–52], who verified a decrease in subsurface demineralization of enamel after irradiation, and attributed this event to a decrease in solubility. Another explanation, it is apatite crystals in dental enamel incorporate sodium, carbonate and magnesium during their formation and irradiation, it would

probably cause punctual defects within the apatite and thus, ions could be removed from the crystal surfaces inside the enamel pores [52].

In addition, a study demonstrated greater expression of matrix metalloproteinase 20 (MMP-20), in the dentin-enamel junction of irradiated teeth. The proteolytic activity of MMP-20 may be responsible for the degradation of the structure of non-collagenous proteins, such as amelogenin and ameloblastin, located in the organic matrix of enamel, leading to delamination of this tissue and contributing to the etiology of RRC [35–37,53–56].

The interaction between radiation and water is high in dentin [57]. The radiolysis process releases H + and OH- ions into the environment, which can interact with other ions and produce new compounds. This fact explains the decrease in C ions and the lower values of Ca/P weight after exposure to radiation. These ions could induce the formation of a secondary non-apatite calcium phosphate phase, which would make the tissue more susceptible to degradation [58], even for long period of time [57], a fact that would justify the increased risk of developing RRC and/or fractures in the dentin structure

Velo (2018) [59] observed the incorporation of magnesium (Mg) after irradiation with 55 and 70Gy. Mg as a substituent component inhibits crystal growth and strongly influences the lattice parameters, which may have made the apatite amorphous. This change favors the occurrence of a less well-structured crystal arrangement, increasing the permeability and susceptibility of this substrate to cracks, contributing to the obliteration of dentinal tubules [60]. These structural defects can make dentin dry and friable [24], in addition to xerostomia that can occur [61], these changes would act synergistically as factors for the occurrence of RRC.

The clinical extrapolation of the results must be cautious, because, despite being reproduce, as much as possible, it is not possible to fully mimic what actually occurs in the living organism [21,33,62]. However, in vitro studies allow the standardization not only of samples, but also of experimental conditions, which would be extremely difficult to achieve in in vivo studies, both due to the nature of the study and the clinical and emotional conditions of the patients. Thus, research conducted with this study model is necessary and contributes to the understanding of the effects of RT on dental tissues, and can contribute to clinical repercussions on patients.

In this way, through the results obtained, this study contributes to the evaluation, quantification and understanding of the direct effects of RT on dental tissues and suggest that the toxicity caused by radiation to dental enamel is even greater and more complex in cases of re-irradiation, being of it is fundamentally important to expand knowledge about the effects caused by additional doses used in cases of retreatment, often above the tolerance doses of irradiated tissues.

CONCLUSION

Re-irradiation caused progressive chemical and morphological changes in the enamel and dentin with the escalation of radiation doses. The changes generated by RT on the composition of the teeth are

directly proportional to the dose administered and are more severe after re-irradiation.

DECLARATIONS

Data availability

No new data were generated or analyzed for this editorial.

Author contributions

TTS (Writing – original draft, Investigation, Methodology), VSM (Formal analysis, Writing – review & editing), KFM (Writing – review & editing), FWGPS (Formal analysis), HFO (Resources), JJF (Formal analysis), PNF (Formal analysis), JCCN (Supervision, Formal analysis), RGPD (Resources), AMQ (Conceptualization; Writing – original draft, Supervision).

Funding

No funding was received to assist with the preparation of this manuscript.

Conflicts of interest

The authors have no conflicts of interest to declare that are relevant to the content of this article.

REFERENCES

1. García-Anaya MJ, Segado-Guillot S, Cabrera-Rodríguez J, Toledo-Serrano MD, Medina-Carmona JA, Gómez-Millán J. Dose and volume de-escalation of radiotherapy in head and neck cancer. *Crit Rev Oncol Hematol*. 2023;186:103994. doi:10.1016/j.critrevonc.2023.103994
2. Steel GG, McMillan TJ, Peacock JH. The 5Rs of radiobiology.Int J Radiat Biol. 1989; 56:1045-48.
3. Harrington K, Nutting C, Newbold K, Bhide S. Principles and practice of head and neck surgery and oncology. Chapman and Hall – CRC. 2009.
4. Douchy L, Gauthier R, Abouelleil-Sayed H, Colon P, Grosgogeat B, Bosco J. The effect of therapeutic radiation on dental enamel and dentin: A systematic review. *Dent Mater*. 2022;38(7):e181-e201. doi:10.1016/j.dental.2022.04.014
5. Toletino E, Centurion B, Ferreira L, de Souza A, Damante JH, Rubiea-Bullen IR. Oral adverse effects of head and neck radiotherapy: literature review and suggestion of a clinical oral care guideline for irradiated patients. J Appl Oral Sci. 2011; 19(5): 448-54.
6. Nayak SG, Pai MS, George LS. Quality of life of patients with head and neck cancer: A mixed method study. *J Cancer Res Ther*. 2019;15(3):638-644. doi:10.4103/jcrt.JCRT_1123_16
7. Hinds PS, Birenbaum LK, Clarke-Steffen L, Quargnenti A, Kreissman S, Kazak A, Meyer W, Mulhern R, Pratt C, Wilimas J. Coming to terms: Parents' response to a first cancer recurrence in their child. Nursing Research. 1996; 45(3):148-53.

8. Vivar CG, Canga N, Canga AD, Arantzamendi M. The psychosocial impact of recurrence on cancer survivors and family members: A narrative review. Journal of Advanced Nursing. 2009; 65(4):724-736.
9. Devita JR VT, Lawrence TS, Rosenber S. Cancer: Principles and practice of Oncology. Pennsylvania: Lippincott Williams &Wilkins. 2011.
10. Naidu MUR, Ramana GV, Rani PU, Mohan Iyyapu K, Suman A, Roy P. Chemotherapy-induced and/or radiation therapy induced oral mucositis-complicating the treatment of cancer. Neoplasia. 2004; 6:423-31.
11. Bensadoun RJ, Riesenbeck D, Lockhart PB, Elting LS, Spijkervet FKL, Brennan MT, et al. A systematic review of trismus induced by cancer therapies in head and neck cancer patients. Support Care Cancer. 2010; 18:1033-38.
12. Epstein JB, Stevenson-Moore, P. Periodontal disease and periodontal management in patients with cancer. Oral Oncol. 2001; 37:613-19.
13. Nabil S, Samman N. Incidence and prevention of osteoradionecrosis after dental extraction in irradiated patients: a systematic review. Int J Oral Maxillofac Surg. 2011; 40:229-243.
14. Siripamitdul P, Sivavong P, Osathanon T, et al. The Effects of Radiotherapy on Microhardness and Mineral Composition of Tooth Structures. *Eur J Dent*. 2023;17(2):357-364. doi:10.1055/s-0042-1746414
15. Pistoia AD, Pistoia GD, Neto MM, Hahn D, Rigodanzo L. Manifestações bucais decorrentes do tratamento antineoplásico. Revista de Dentística. 2004; 3(9).
16. Ferguson DMD, Stevens MR. Advances in Head and Neck Radiotherapy to the Mandible. Oral and Maxillofacial Surgery Clinics of North America. 2007; 19:553-63.
17. Hong CHL, Napeñas JJ, Hodgson BD, Stokman MA, Mathers-Stauffer M, Elting LS, *et al.* A systematic review of dental disease in patients undergoing cancer therapy. Support Care Cancer. 2010; 18:1007-21.
18. Mc Caul LK. Oral and Dental Management for Head and Neck Cancer Patients Treated by Chemotherapy and Radiotherapy. Dental Update. 2012; 39:135-40.
19. Khaw A, Logan R, Keefe D, Bartold M. Radiation-induced oral mucosites and periodontitis – proposal for inter-relationship. Oral Diseases. 2014; 20(3):7-18.
20. Andrews N, Griffiths C. Dental complications of head and neck radiotherapy: Part 1. Aust Dent J. 2001; 46(2): 88-94.
21. Germano F, Melone P, Testi D, Arcuri L, Marmiroli L, Petrone A, et al. Oral complications of head and neck radiotherapy: prevalence and management. Minerva Stomatol. 2015; 64(4):189-202.
22. Gwinnett AJ. Structure and composition of enamel. Oper Dent. 1992; 5(5):10–7.
23. De Siqueira Mellara T, Palma-Dibb RG, de Oliveira HF, Garcia Paula-Silva FW, Nelson-Filho P, da Silva RA, da Silva LA, de Queiroz AM. The effect of radiation therapy on the mechanical and

morphological properties of the enamel and dentin of deciduous teeth – an *in vitro* study. Radiation Oncology. 2014; 22(9):30.

24. Gonçalves LMN, Palma-Dibb RG, Paula-Silva FW, Oliveira HF, Nelson-Filho P, Silva LA, Queiroz AM. Radiation therapy alters micro hardness and microstructure of enamel and dentin of permanent human teeth. Journal Dent. 2014; 42(8):986-92.
25. Marangoni-Lopes L, Rovai-Pavan G, Steiner-Oliveira C, Nobre-dos-Santos M. Radiotherapy Reduces Microhardness and mineral and organic composition and Changes the Morphology of Primary Teeth: an *in vitro* study. Caries Res. 2019; 53(3):296-304.
26. Mellara TS, Paula-Silva FWG, Arid J, de Oliveira HF, Nelson-Filho P, Bezerra Silva RA, Torres FM, Faraoni JJ, Palma-Dibb RG, de Queiroz AM. Radiotherapy Impairs Adhesive Bonding in Primary Teeth: An In Vitro Study. J Dent Child (Chic). 2020; 87(2):69-76.
27. Grötz KA, Duschner H, Kutzner J, Thelen M, Wagner W. Histotomography studies of direct radiogenic dental enamel changes. Mund Kiefer Gesichtschir. 1998;2(2):85–90.
28. Kielbassa AM, Beetz I, Schendera A, Hellwig E. Irradiation effects on microhardness of fluoridated and non-fluoridated bovine dentin. Eur J Oral Sci. 1997; 105(5-1)444-7.
29. Walker MP, Wichman B, Cheng AL, Coster J, Williams KB. Impact of Radiotherapy Dose on Dentition Breakdown in Head and Neck Cancer Patients. *Pract Radiat Oncol*. 2011;1(3):142-148. doi:10.1016/j.prro.2011.03.003
30. Soares CJ, Castro CG, Neiva NA, Soares PV, Santos-Filho PC, Naves LZ, Pereira PN. Effect of gamma irradiation on ultimate tensile strength of enamel and dentin. J Dent Res. 2010;89(2):159-64.
31. Jervoe P. X-ray diffraction investigation on the effect of experimental and in situ radiation on mature human teeth. A preliminary report. Acta Odontol Scand. 1970; 28(5):623–31.
32. Fränzel W, Gerlach R. The irradiation action on human dental tissue by X-rays and electrons – a nanoindenter study. Z Med Phys. 2009; 19(1):5–10.
33. Kielbassa AM. In situ induced demineralization in irradiated and non-irradiated human dentin. Eur J Oral Sci. 2000; 108(3):214-21.
34. Springer IN, Niehoff P, Warnke PH, Böcek G, Kovács G, Suhr M, Wiltfang J, Açil Y. Radiation caries--radiogenic destruction of dental collagen. Oral Oncol. 2005 Aug;41(7):723-8.
35. McGuire JD, Mousa AA, Zhang BJ, Todoki LS, Huffman NT, Chandrababu KB, Moradian Oldak J, Keightley A, Wang Y, Walker MP, Gorski JP. Extracts of irradiated mature human tooth crowns contain MMP-20 protein and activity. J Dent. 2014; 42(5):626-35.
36. Queiroz AM, Bonilla CMC, Palma-Dibb RG, et al. Radiotherapy Activates and Protease Inhibitors Inactivate Matrix Metalloproteinases in the Dentinoenamel Junction of Permanent Teeth. *Caries Res*. 2019;53(3):253-259. doi:10.1159/000492081
37. Queiroz AM, Carpio-Bonilla CM, Arnez MFM, Dos Santos TT, Palma-Dibb RG, Oliveira HF, Nelson-Filho P, Silva LAB, Paula-Silva FWG. Radiotherapy Activates Matrix Metalloproteinases in the Dentinoenamel Junction of Primary Teeth. J Dent Child (Chic). 2020 May 15;87(2):83-89.

38. Jansma J, Vissink A, Jongebloed WL, Retief DH, Johannes S, Gravenmade E. Natural and induced radiation caries: A SEM study. Am J Dent. 1993; 6(3):130-6.
39. Al-Nawas B, Grotz KA, Rose E, Duschner H, Kann P, Wagner W. Using ultrasound transmission velocity to analyse the mechanical properties of teeth after in vitro, in situ, and in vivo irradiation. Clin Oral Investig. 2000; 4(3):168-72.
40. Soares CJ, Neiva NA, Soares PB, Dechichi P, Novais VR, Naves LZ, Marques MR. Effects of chlorhexidine and fluoride on irradiated enamel and dentin. J Dent Res. 2011; 90(5):659-64.
41. Bulucu B, Avsar A, Demiryurek EO, Yesilyurt C. Effect of radiotherapy on the microleakage of adhesive systems. J Adhes Dent. 2009; 11(4):305-9.
42. Martins CV, Leoni GB, Oliveira HF, Arid J, Queiroz AM, Silva LAB, Sousa-Neto MD. Influence of therapeutic cancer radiation on the bond strength of an epoxy- or an MTA-based sealer to root dentine. Int Endod J. 2018; 49(11):1065-1072.
43. Santin GC, Palma-Dibb RG, Romano FL, Oliveira HF, Nelson-Filho P, de Queiroz AM. Physical and adhesive properties of dental enamel after radiotherapy and bonding of metal and ceramic brackets. Am J Orthod Dentofacial Orthop. 2015; 148(2):283-92.
44. Gale MS, Darvel BW. Thermal cycling procedures for laboratory testing of dental restorations. J Dent. 1999; 27: 89-99.
45. Li J, Choo-Smith LP, Tang Z, Sowa MG. Background removal from polarized Raman spectra of tooth enamel using the wavelet transform. Journal of Raman Spectroscopy. 2010; 42(4):580-85.
46. Reed R, Xu C, Liu Y, Gorski JP, Wang Y, Walker MP. Radiotherapy effect on nano-mechanical properties and chemical composition of enamel and dentine. Archives of Oral Biology. 2015; 60(5):690–697.
47. Timchenko EV, Timchenko PE, Volova LT, Rosenbaum AY, Kulabukhova AY. Analysis of tooth tissues using Raman spectroscopy. Journal of Physics: Conference Series. 2016; 769, 012047.
48. Lu H, Zhao Q, Guo J, et al. Direct radiation-induced effects on dental hard tissue. *Radiat Oncol*. 2019;14(1):5. Published 2019 Jan 11. doi:10.1186/s13014-019-1208-1
49. Madrid CC, de Pauli Paglioni M, Line SR, et al. Structural Analysis of Enamel in Teeth from Head-and-Neck Cancer Patients Who Underwent Radiotherapy. Caries Res. 2017;51(2):119-128. doi:10.1159/000452866
50. Joyston-Bechal S. The effect of X-radiation on the susceptibility of enamel to an artificial caries-like attack in vitro. J Dent. 1985; 13(1):41-4.
51. Jansma J, Buskes JA, Vissink A, Mehta DM, Gravenmade EJ. The effect of X-ray irradiation on the demineralization of bovine dental enamel. A constant composition study. Caries Res. 1988; 22(4):199-203.
52. Jansma J, Borggreven JM, Driessens FC, Gravenmade EJ. Effect of X-ray irradiation on the permeability of bovine dental enamel. Caries Res. 1990; 24(3):164-8.

53. Hübner W, Blume A, Pushnjakova R, Dekhtyar Y, Hein HJ. The influence of X-ray radiation on the mineral/organic matrix interaction of bone tissue: an FT-IR microscopic investigation. Int J Artif Organs. 2005; 28(1):66-73.
54. Mitchell MJ, Logan PM. Radiation-induced changes in bone. Radiographics 1998; 18(5):1125-113
55. Kielbassa AM, Hinkelbein W, Hellwig E, Meyer-Lückel H. Radiation-related damage to dentition. Lancet Oncol. 2006; 7(4): 326-35.
56. Yahyazadehfar M, Arola D. The role of organic proteins on the crack growth resistance of human enamel. Acta Biomater. 2015; 19:33-45.
57. Cole T, Silver AS. Production of hydrogen atoms in teeth by X-irradiation. Nature. 1963; 16(200):700-1.
58. Celik EU, Ergücü Z, Türkün LS, Türkün M. Effect of different laser devices on the composition and microhardness of dentin. Oper Dent. 2008; 33(5):491–496.
59. Velo MMAC, Farha ALH, da Silva Santos PS, Shiota A, Sansavino SZ, Souza AT, Honório HM, Wang L. Radiotherapy alters the composition, structural and mechanical properties of root dentin in vitro. Clin Oral Investig. 2018; 22(8):2871-2878.
60. Brannstrom M. The hydrodynamic theory of dentinal pain: sensation in preparations, caries, and the dentinal crack syndrome. *J Endod*. 1986;12(10):453-457. doi:10.1016/S0099-2399(86)80198-4
61. Craddock HL. Treatment and maintenance of a dentate patient with ‘radiation caries’. Dent Update. 2006; 33(8):462–68.
62. Morais-Faria K, Menegussi G, Marta G, Fernandes PM, Dias RB, Ribeiro AC, Lopes MA, Cernea CR, Brandão TB, Santos-Silva AR. Dosimetric distribution to the teeth of patients with head and neck cancer who underwent radiotherapy. Oral Surg Oral Med Oral Pathol Oral Radiol. 2015; 120(3):416-9.

Figures

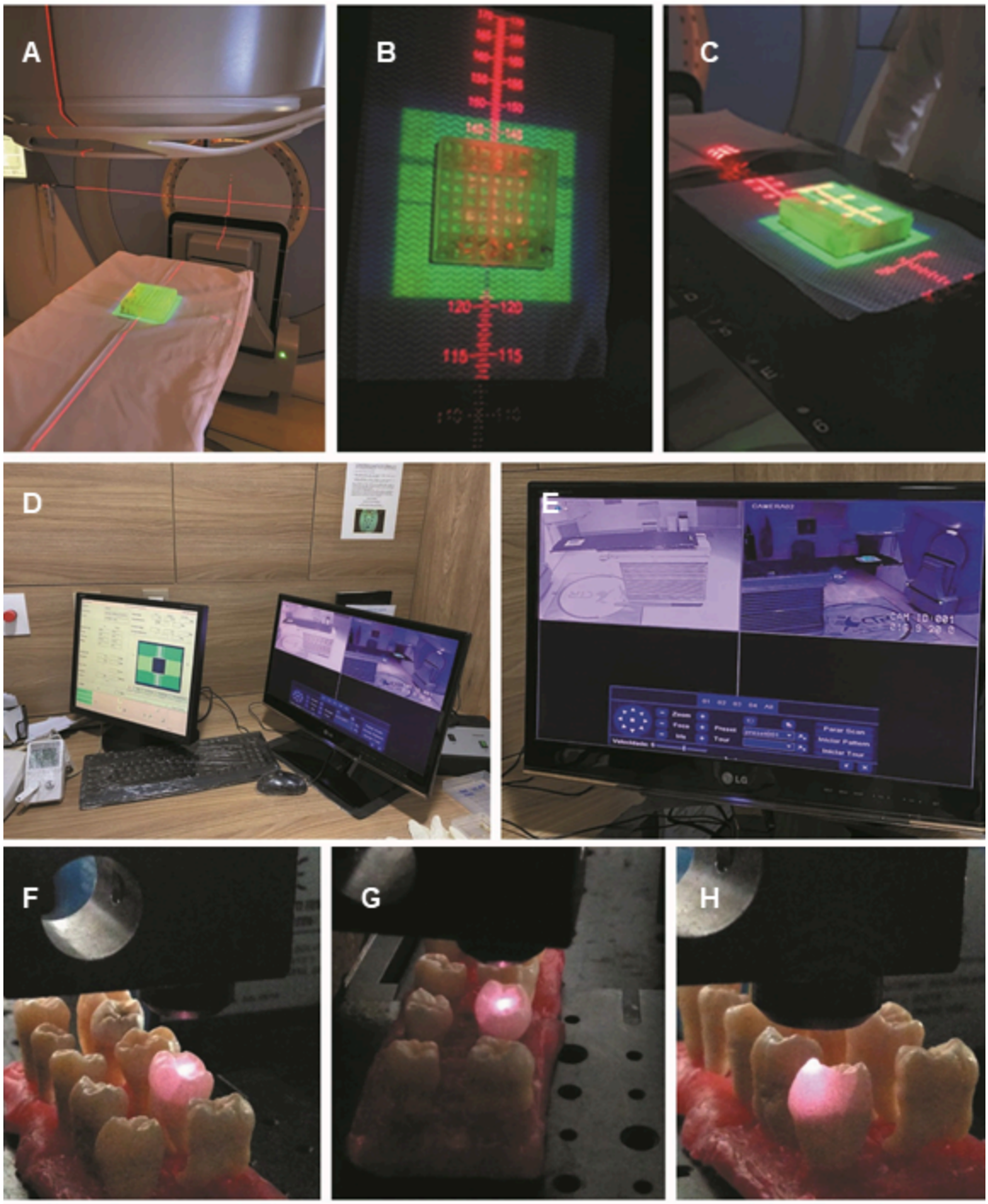

Figure 1

A-E Irradiation and re-irradiation process of teeth in a linear accelerator. F-H Raman Spectroscopy process.

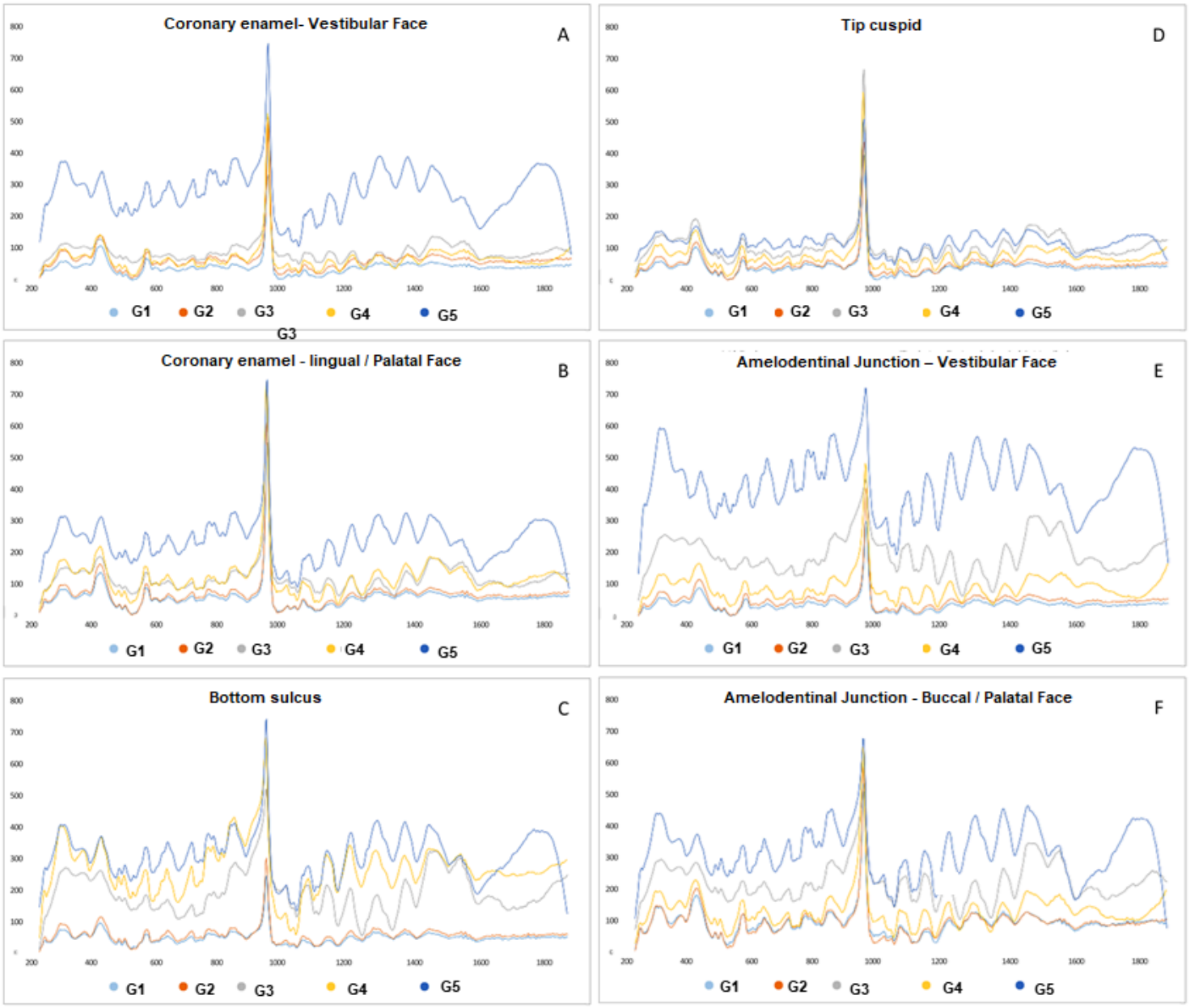

Figure 2

Average spectra for each of the regions analyzed, according to each group. Of which: A – Coronary Enamel – Vestibular Face ; B – Coronary Enamel – Lingual/Palatal Face; C – Bottom sulcus; D – Tip cuspid; E – Amelodentinal Junction – Vestibular Face; F – Amelodentinal Junction – Buccal / Palatal.

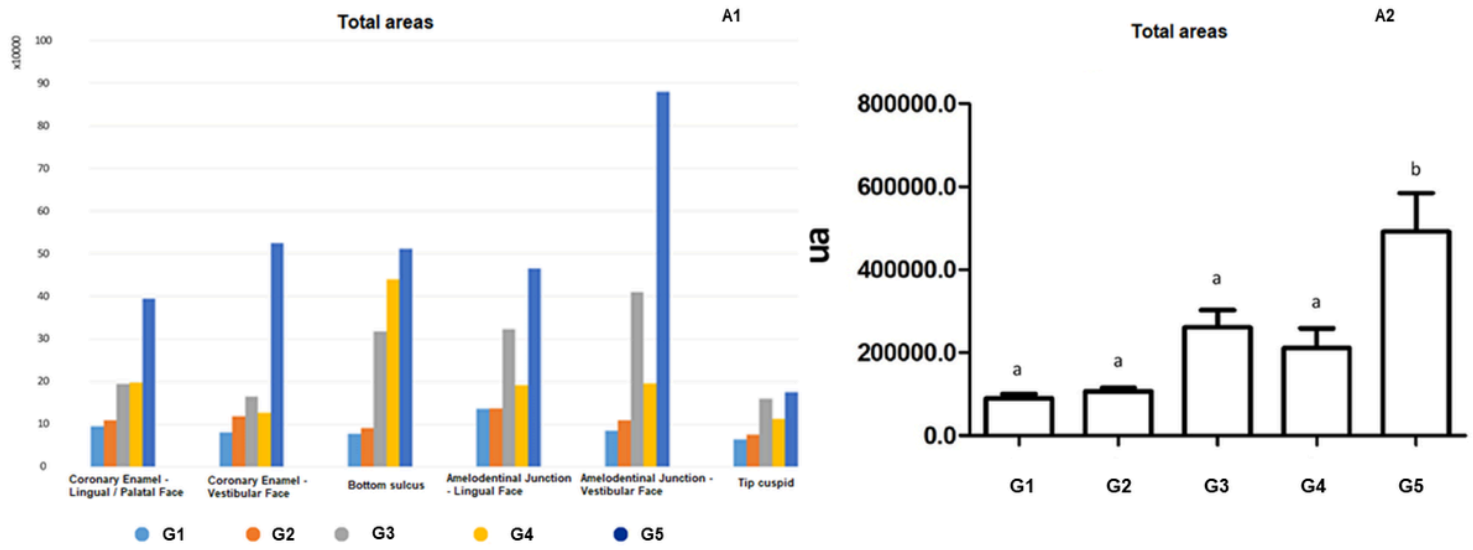

Figure 3

Graphical representation of total spectra areas for each group and region analyzed and the measurements of the total areas of the spectrum peaks. Values expressed in arbitrary units (ua). Different letters mean statistically significant difference (p>0.005).

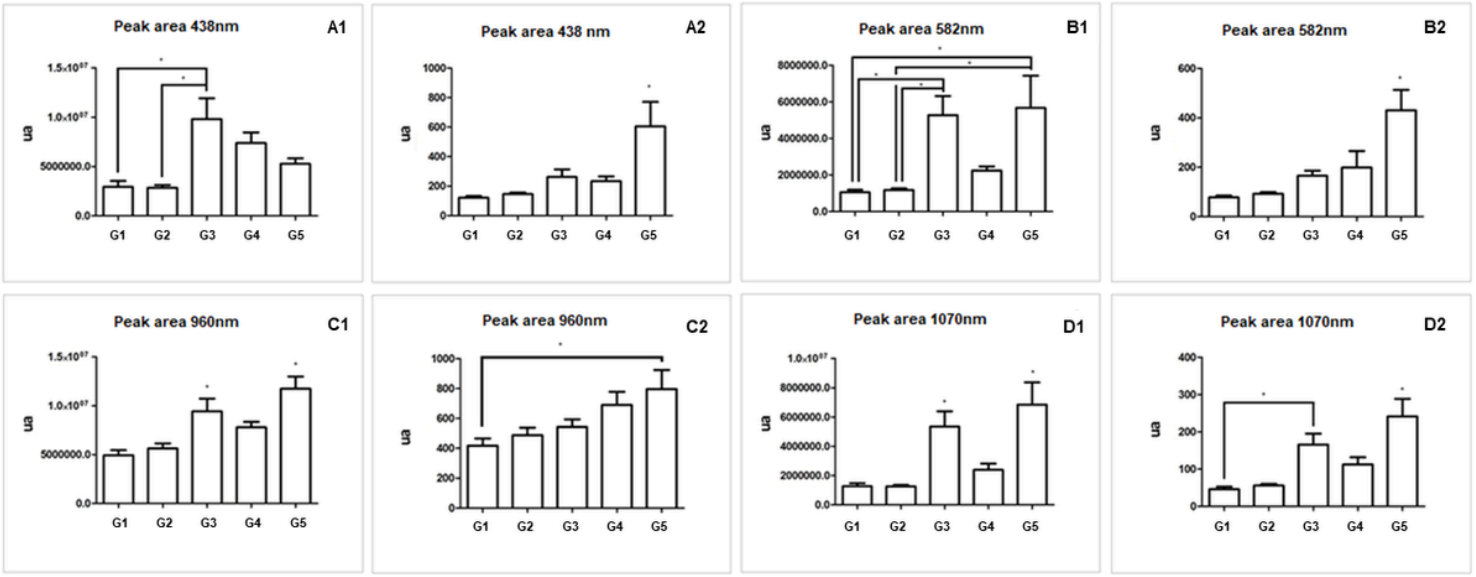

Figure 4

Area values for the selected peaks in each region, for each groups. A1 – peak area 438nm; B1 – peak area 582nm; C1 – peak area 960nm; D1 – 1070nm peak area. And graphical representation of the area measurements of the selected peaks. Values expressed in arbitrary units (ua). Asterisk (*) indicates statistically significant difference (p>0.005).

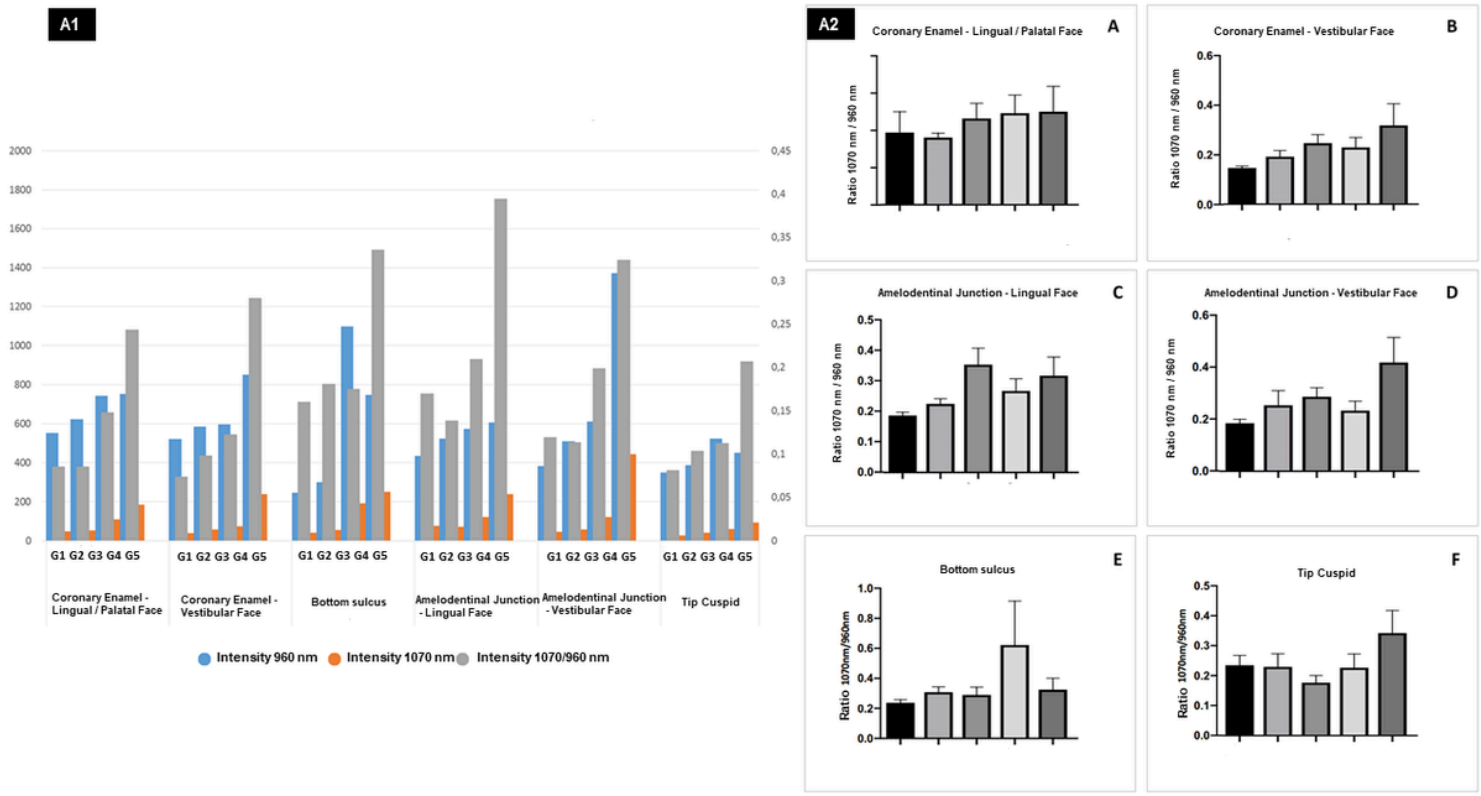

Figure 5

A1: Value for the intensity of the peaks at 960nm, 1070nm and the ratio (1070/960). A2: Graphical representation of the ratio (1070/960), for each region and according to each sample group. Values expressed in arbitrary units (ua). Asterisk (*) indicates statistically significant difference (p>0.005).

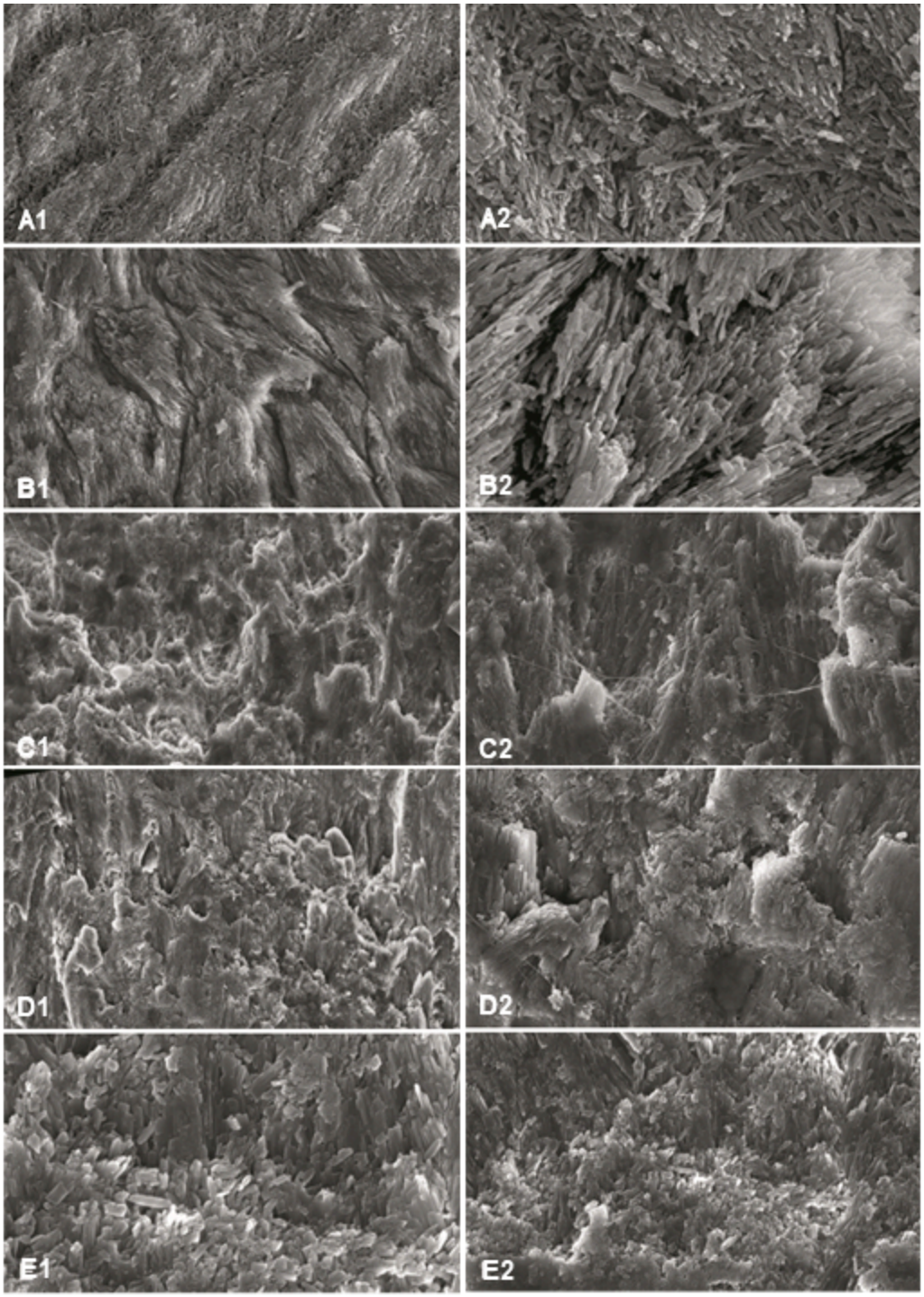

Figure 6

Electron micrographs of the enamel of permanent teeth, obtained using scanning electron microscopy, at 5000x magnification (A1, B1, C1, D1, E1) and 20,000x (A2, B2, C2, D2, E2): (A1 and A2): G1 group - non-irradiated enamel with the presence of well-organized prisms surrounded by interprismatic regions; (B1 and B2): G2 group - enamel irradiated up to a dose of 60Gy, with evidence of the interprismatic region, without difficulty in observing the prisms and crystals; (C1 and C2): G3 group- re-irradiated up to a dose of 30Gy; (D1 and D2): G4 group - re-irradiated up to a dose of 40Gy; and (E1 and E2): G5 group - re-

irradiated up to a dose of 50Gy – progressive morphological changes, with the escalation of radiation doses, with loss of visibility of the interprismatic region and difficulty in observing prisms and crystals.

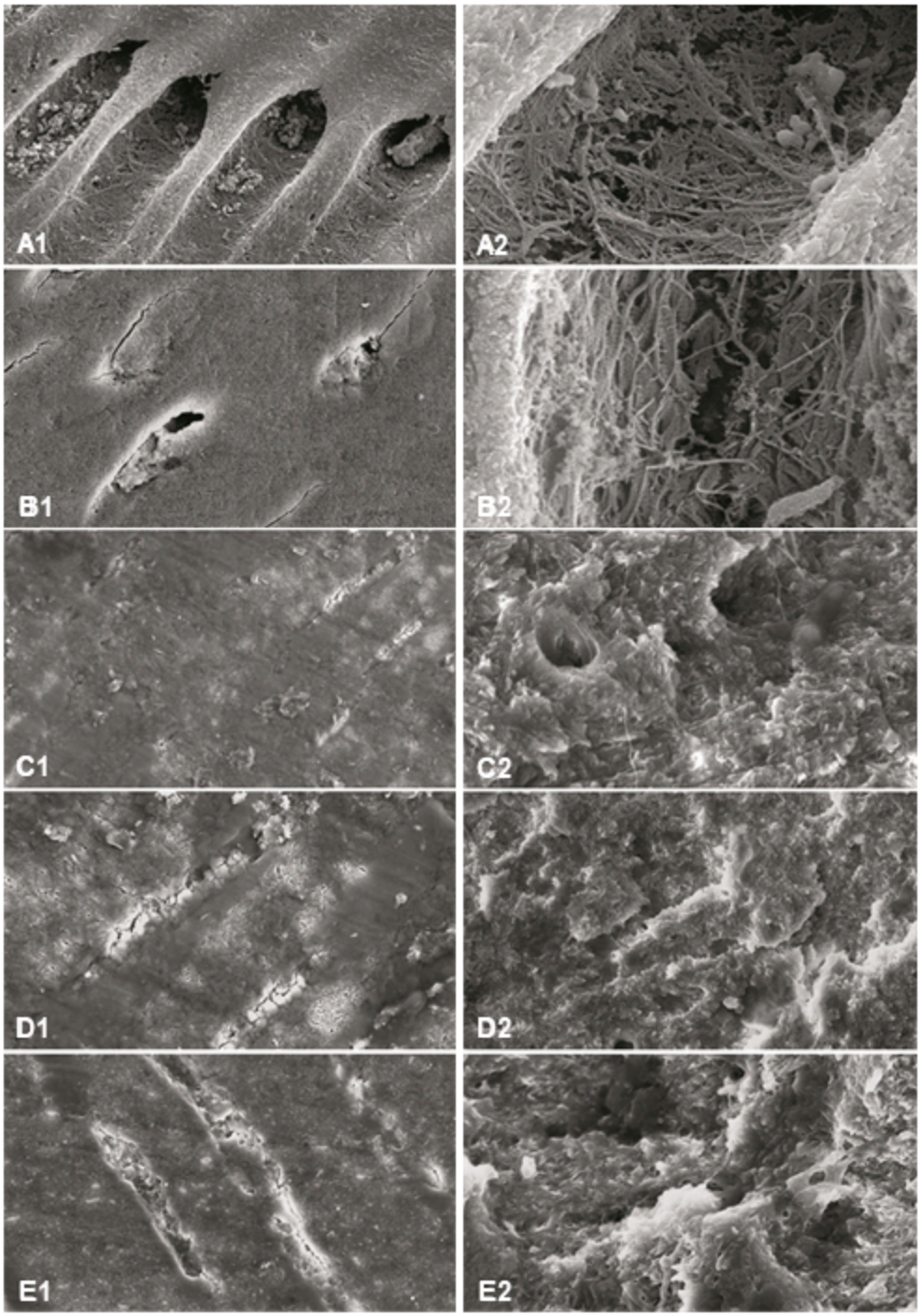

Figure 7

Electron micrographs of the dentin of permanent teeth, obtained using scanning electron microscopy, at 5000x (A1, B1, C1, D1, E1) and at 20,000x magnification (A2, B2, C2, D2, E2): (A1 and A2): non-irradiated dentin with the presence of defined dentinal tubules and a network of organized collagen fibers; (B1 and B2): dentin irradiated up to 60Gy, with alteration of the intertubular, peritubular and intratubular dentin; presence of cracks in the dentin structure and collapsed and/or destroyed dentinal tubules; (C1 and C2): dentin re-irradiated up to a dose of 30Gy, (D1 and D2): dentin re-irradiated up to a dose of 40Gy, (E1 and

E2): dentin re-irradiated up to a dose of 50Gy – progressive morphological changes, with the escalation of radiation dose, with degradation of the intertubular, peritubular and intratubular structure, presence of cracks in the structure, obstruction of dentinal tubules and degradation of collagen fibers.